Modelling acoustic emissions generated by sliding friction

Yibo Fan*, Fengshou Gu, Andrew Ball

School of Computing and Engineering, The University of Huddersfield, Queensgate, Huddersfield, HD1 3DH, UK

ARTICLE INFO

ABSTRACT

Acoustic emission analysis is an effective diagnostic method in modern tribo-monitoring. Many experimental studies have been conducted to investigate the relationship between AE parameters and wear and friction. This paper develops a theoretical model to correlate acoustic emissions to sliding friction based on elastic asperity contact of materials. It is found that sliding speed, load supported by asperities, the number of asperity contact and surface topographic characteristics influence the energy of AE signal. With the help of this model it is possible to estimate the contact load supported by asperities from AE measurement, which is a critical parameter to evaluate lubrication conditions in engineering applications. The establishment of this model will provide a theoretical basis for future studies on the motioning and prognostics of tribological process using AE technology.

© 2009 Elsevier B.V. All rights reserved.

1. Introduction

As an attractive method, acoustic emission (AE), the transient elastic wave that is spontaneously generated from a rapid release of strain energy, has been widely investigated to monitor the sliding wear and friction. Boness and McBride [1] found that asperity contact between the sliding surfaces was the primary source of acoustic emissions. When the surfaces were completely separated by lubricating film, no AE signal above the noise level could be detected. They also established an empirical relationship between the integrated RMS value of AE signal and the wear volume removed from the test ball in a steel-on-steel sliding test. This relationship was confirmed later by the tests conducted under different conditions [2,3].

Attempts to correlate the AE time domain parameters with the wear process were also made by other research. Lingard et al. [4] found that there was a systematic relationship between cumulative AE counts and the wear volume for typical wear tests. Matsuoka et al. [5] developed a model to correlate the AE RMS value with the material removal power in wear process. Based on this model, they demonstrated that the wear coefficient could be estimated and monitored on-line by measuring AE RMS through an abrasive wear test of magnetic recording head materials.

Except for the quantitative prediction of the wear process, the AE technique was also found to be a sensitive method to indicate different friction and wear mechanisms. Lingard et al. [4] found that the AE count rate was more sensitive to the contact condition than either the wear rate or the friction force in a pure sliding test on metallic specimens. Their study also showed that the weighted count rate could indicate the variation of friction coefficient in different lubrication regimes. Hanchi and Klamecki [6] investigated the AE activities in a serial metallic pin-on-disk contact tests and concluded that the AE count rate, together with AE amplitude distribution and AE energy, had a strong potential for the identification of the mild-severe wear transition. Correlation between the AE count rate, AE RMS value and the coefficient of friction, the transition of wear mechanism was also found in other studies [3,7].

With the wide application of ceramics, AE monitoring of ceramic sliding friction attracted more and more attention. Wang and Wood [8] showed that there was a correlation between instantaneous AE RMS signal and the coefficient of friction in an experimental study on oil lubricated hybrid sliding friction between ceramics and metals. Studies on ceramic mechanical seals [9] found that the lubrication condition at sealing interface could be indicated by measuring the RMS value of AE signal.

These previous studies show that there is a good correlation between friction or wear and the energy of AE signal, no matter whether the AE energy is characterized by AE counts or RMS. Empirical models were even established on the basis of experimental research. But there is a lack of theoretical model to reveal the relationship between AE measurement and friction and very few works in this field have been published.

This paper attempts to fill this gap and presents a model to correlate the energy of acoustic emissions to sliding friction on the basis of the elastic asperity contact of materials. With the help of this model, it is possible to evaluate the severity of asperity contract through AE measurement. Since the control of asperity contact load is critical in many engineering applications such as the

---

* Corresponding author. Fax: +44 01484421106.
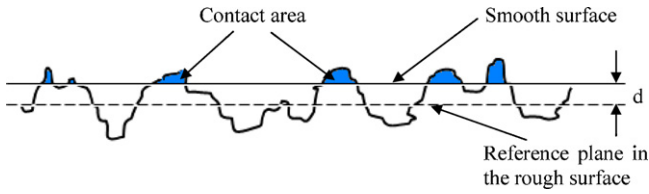 *E-mail address:* y.fan@hud.ac.uk (Y. Fan).

Fig. 1. Contacts of a smooth surface and a rough surface.

lubrication of mechanical seals, this model will provide a powerful tool to the development of AE prognostics to detect and evaluate the premature failure of machinery at an early stage.

2. The AE model of elastic asperity contacts

2.1. AE generated by sliding friction

When two solid bodies contact, the true contact areas distributed between numbers of asperities due to surface roughness are an extremely small portion of the apparent contact area. These true contact areas rather than the apparent contact area have a decisive effect on the wear and friction. Hence the control of asperity contacts is critical to avoid excessive friction and wear in engineering practice.

It has been found that asperity contact was the main AE source in sliding friction [1]. High frequency stress waves can be released due to the elastic or plastic deformation of asperities, fracture of asperities or the adhesion between asperities, and the possible plough, cutting and grooving. According to the plastic-junction theory of sliding friction developed by Bowden and Tabor [10], all contacting asperities deformed plastically even under weak normal pressure because of high local stress. The pressure undertaken by each plastic junction is constant and thus the real contact area is proportional to the load. However, Archard [11] pointed out in a later research that the deformation of asperities could be largely elastic in highly finished or well running-in surfaces. By modelling a rough surface covered by a hierarchy of asperities, the proportionality between the load and contact area could be successfully approximated when multiple stages of elastic contact are considered. Therefore it has practical meaning to model the AE signal generated by the elastic deformation of contacting asperities in sliding friction.

2.2. Elastic energy generated by asperity contact

The contact of two engineering flat surfaces with roughness R_{q1} and R_{q2} can be analysed by converting it to the contact between an ideal plane and a flat surface with roughness $R'_q = \sqrt{R_{q1}^2 + R_{q2}^2}$. To simplify the modelling, all the asperity summits are assumed to be spherical and have the same radius. Their heights vary randomly, denoted by random variable z.

Fig. 1 shows schematically the contact between a rough flat surface and a smooth plane. The load is supported by those asperities whose heights are greater than the separation between the reference planes. The probability that a particular asperity has a height between z and $z + dz$ above the reference plane is,

$$P(z) = f(z)dz \tag{1}$$

where $P(z)$ is the probability; $f(z)$ is the probability density function (PDF) of the asperity height.

Assume the separation of the smooth plane and the reference plane in the rough surface is d. It can be seen from Fig. 1 that all the asperities with a height in excess of d would contact with the smooth surface and support the load. So the probability of making contact at any selected asperity can be expressed as [12]

$$P(z > d) = \int_d^\infty f(z)dz \tag{2}$$

If the number of asperities per unit area is D_{SUM}, the expected number of contacts in any unit area is

$$n = D_{SUM} \int_d^\infty f(z)dz \tag{3}$$

For the contact of a pair of asperities, the stored elastic energy (U_{iE}) can be expressed as [13]

$$U_{iE} = \int W d\delta \tag{4}$$

where W is the normal load; $\delta = z - d$, is the maximum deflection of asperity in the contact area:

$$\delta = \left(\frac{W^2}{E'^2 R'} \right)^{1/3} \tag{5}$$

E' is the Hertzian contact modulus given by

$$\frac{1}{E'} = \frac{3}{4} \left(\frac{1 - v_1^2}{E_1} + \frac{1 - v_2^2}{E_2} \right) \tag{6}$$

E_1, E_2 are the Yong's modulus of the contact materials; v_1, v_2 are the Poisson's ratios of the contact materials; R' is Hertzian curvature. Since the contact is between an asperity and a plan, R' is the radius of the asperity.

Substitute Eq. (5) into Eq. (4), then

$$\begin{aligned} U_{iE} &= \frac{2}{3E'^{2/3}R'^{1/3}} \int W^{2/3} dW \\ &= \frac{2W^{5/3}}{5E'^{2/3}R'^{1/3}} = \frac{2}{5}W\delta \end{aligned} \tag{7}$$

Since $\delta = z - d$, the mean elastic energy of one asperity contact is

$$\overline{U_{iE}} = \frac{2\int_d^\infty W\delta f(z)dz}{5\int_d^\infty f(z)dz} = \frac{2\int_d^\infty W(z-d)f(z)dz}{5\int_d^\infty f(z)dz} \tag{8}$$

So the total elastic energy stored in the asperity contacts (U_E) will be

$$U_E = A_o n \overline{U_{iE}} \tag{9}$$

where A_o is the apparent contact area; n is the number of contacts in unit area given by Eq. (3).

Using Eqs. (3) and (8), the total elastic energy can be given by

$$U_E = 0.4 A_o D_{SUM} W \int_d^\infty (z - d)f(z)dz \tag{10}$$

If the velocity of the surface sliding is v, then the time needed for the release of individual asperity contact can be expressed as

$$\tau = \frac{a}{v} \tag{11}$$

where a is the Hertzian radius of the asperity contact circle given by

$$a = \left(\frac{WR'}{E'} \right)^{1/3} \tag{12}$$

Substituting Eq. (12) into Eq. (11)

$$\tau = \frac{a}{v} = \frac{(WR')^{1/3}}{E'^{1/3}v} = \frac{(\delta R')^{1/2}}{v} \tag{13}$$

Using $\delta = z - d$, the mean release time of asperity contact is

$$\bar{\tau} = \frac{\int_d^\infty R'^{1/2}\delta^{1/2}f(z)dz}{v\int_d^\infty f(z)dz} = \frac{\int_d^\infty R'^{1/2}(z-d)^{1/2}f(z)dz}{v\int_d^\infty f(z)dz} \tag{14}$$

Using Eqs. (10) and (14), the release rate of elastic energy can be expressed as

$$\dot{U}_E = \frac{U_E}{\bar{\tau}} = \frac{0.4A_oD_{SUM}Wv\int_d^\infty(z-d)f(z)dz\int_d^\infty f(z)dz}{R'^{1/2}\int_d^\infty(z-d)^{1/2}f(z)dz} \tag{15}$$

Define the total number of asperity contacts between the two surfaces (N) as

$$N = A_oD_{SUM}\int_d^\infty f(z)dz \tag{16}$$

Define

$$F_n(h) = \int_t^\infty (s-h)^n\phi(s)ds \tag{17}$$

where $h = d/\sigma$, is the standardized separation; σ is the standard deviation of height distribution; $\phi(s)$ is the standardized height distribution

Using Eq. (16) and function $F_n(h)$ defined by Eq. (17), Eq. (15) can be expressed as

$$\dot{U}_E = 0.4NWv\frac{F_1(h)}{R'^{1/2}F_{1/2}(h)} \tag{18}$$

It can be seen from Eq. (18) that the release rate of elastic energy is proportional to the number of asperity contacts and contact load. According to the Greenwood-Williamson model [12], the number of asperities increases linearly along with load. Therefore, there is a square relationship between the elastic energy release rate and contact load. Eq. (18) also shows that the release rate of elastic energy is proportional to the power of contact load and sliding velocity. This is in line with the engineering experience that the Wv value has a strong influence on the sliding friction between two surfaces.

The definition of $F_n(h)$ given by Eq. (17) indicates that $F_n(h)$ is influenced by the surface separation d and the characteristics of surface topography. Research has shown that the separation d is actually also determined by the surface topography and independent of the load applied [12]. Hence, the $(F_1(h))/(R'^{1/2}F_{1/2}(h))$ part in Eq. (18) is only determined by the topographic characteristics of the contact surface.

2.3. The AE model

Suppose that a portion k_e of the elastic strain energy converts to AE pulses and the gain of the AE measurement system is k_m. Using Equation (18), the energy rate of the acoustic emissions generated by asperity contact is given by

$$\dot{U}_{AE} = 0.4k_ek_mNWv\frac{F_1(h)}{R'^{1/2}F_{1/2}(h)} \tag{19}$$

Define $k_c = 0.4k_ek_m$ then Eq. (19) is

$$\dot{U}_{AE} = k_cNWv\frac{F_1(h)}{R'^{1/2}F_{1/2}(h)} \tag{20}$$

Thus the energy collected by AE sensor is
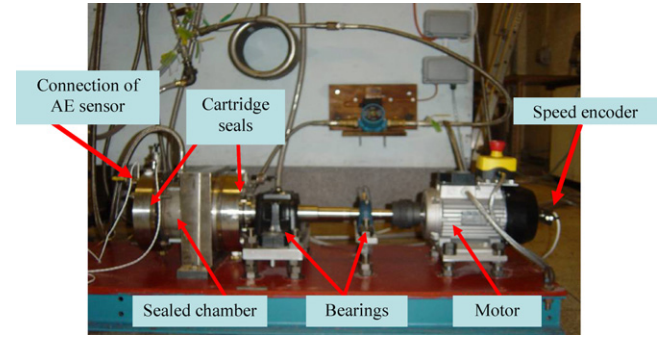
$$U_{AE} = \int_0^\infty \dot{U}_{AE}dt \tag{21}$$

Fig. 2. Layout of the mechanical seal test rig.

This energy equals the energy of the AE signals

$$U_{AE} = G\int_0^\infty V^2(t)dt \tag{22}$$

where G is the electrical conductance of the AE measuring circuit; $V(t)$ is the measured electrical signal

The RMS value of AE signal is defined as

$$V_{rms} = \left[\frac{G}{T}\int_0^T V^2(t)dt\right]^{1/2} = \frac{1}{T}\int_0^T \dot{U}_{AE}dt \tag{23}$$

where T is the selected duration of the AE signal

Assuming the sliding between two surfaces is stable, the elastic energy release rate $\dot{U}_E$ will be constant and a continuous acoustic emission with constant $\dot{U}_{AE}$ will be observed. Using Eqs. (21)–(23), the RMS value of the AE signal excited by the total asperity contact can be expressed as

$$V_{rms} = \sqrt{\dot{U}_{AE}} \tag{24}$$

Substituting Eq. (20) into Eq. (24), the relationship between AE RMS and the elastic sliding of asperity contact can be expressed as

$$V_{rms} = k_sN^{1/2}(Wv)^{1/2}\frac{F_1(h)^{1/2}}{R'^{1/4}F_{1/2}(h)^{1/2}} \tag{25}$$

where

$$k_s = \sqrt{k_c}$$

3. Experimental validation of the AE model

To validate the developed AE model, an experimental study was conducted on the test rig (Fig. 2) designed for the condition monitoring of mechanical seals. Studies conducted by Fan [14] proved that the AE signal measured on the cartridge of mechanical seals was caused by the rubbing between seal faces.

The rig has a pressure chamber at the non-driven end, which consists of two John Crane 1648MP cartridge seals and a stainless steel drum. An auxiliary circulating system is connected with the chamber to pressurize the working fluid (water in this research) and take away the heat generated by the friction of mechanical seal. The load on mechanical seals is able to be changed by adjusting the pressure in the sealed chamber. The shaft of the test rig is driven by an electrical induction motor controlled by an inverter to allow the change of test speed.

The experiment employed the PAC WD2030 sensor with a frequency range from 100 kHz to 1000 kHz. The output of AE sensor was amplified using PAC 2/4/5 preamplifier and sampled using PAC
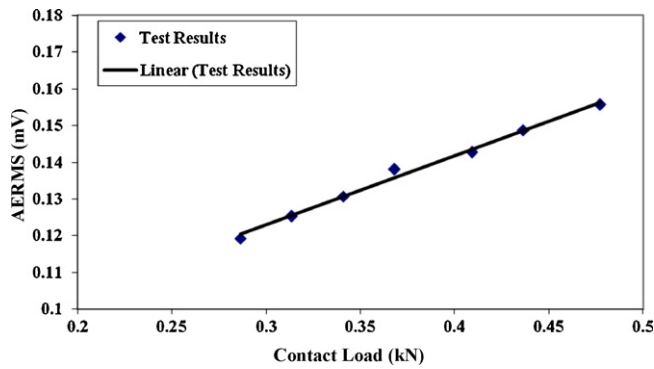
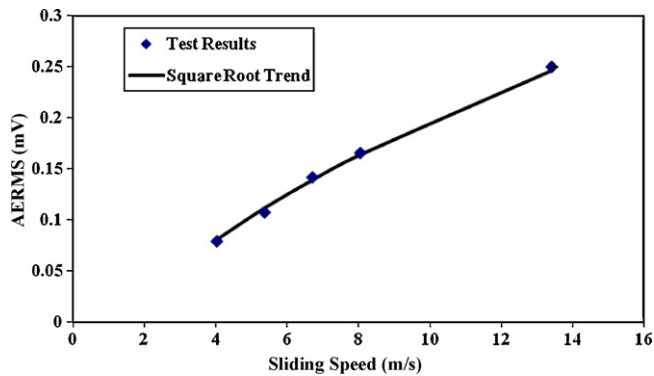**Fig. 3.** AE from mechanical seals running with different contact loads.

Fig. 4. AE from mechanical seals running at different speeds.

PCI 2 data acquisition board. The filter of PAC PCI 2 was set from 100 kHz to 1 MHz and the sampling frequency was 2 MHz. For each test AE raw signal was recorded continuously for 3 s.

The material combination of the tested mechanical seal was reaction-bonded silicon carbide versus antimony-impregnated carbon. The test rig was firstly run at 5 bar and 1500 rpm for 3 h to allow a sufficient running-in of the seal faces. Then the seals were tested at different speeds and pressures to evaluate the influence of sliding speed and contact load on AE signal. The test speeds were 900 rpm, 1200 rpm, 1500 rpm, 1800 rpm and 3000 rpm while the pressure in the sealed chamber was kept at 6 bar. Then the speed of test rig was kept at 1500 rpm and the sealed pressure was increased from 2 bar to 8 bar with the increment of 1 bar. The water temperature was controlled at 26 °C during the tests.

The seal face was lapped to meet the manufacture requirements of John Crane before the test. After the test, the seal face was examined and found that the seal surfaces were well polished due to the running-in. No other wear evidence was observed.

Fig. 3 presents the test results when the seal was run at 1500 rpm with different contact loads. The contact load supported by mechanical seal face was calculated using the well established mechanical performance calculation software available at John Crane UK when different pressure was loaded in the sealed chamber. It can be observed that the relationship between AE RMS value and the contact load is linear ($R^2 = 0.99$) while Eq. (25) predicts that AE RMS is in proportion to the square root of contact load. This is because the influence of contact load (W) on the total number of asperity contact (N) is not taken into account. Since the tested seal was under stable lubrication, the number of asperity contact should increase in proportion to contact load according to Greenwood-Williamson model [12]. Therefore a linear relationship between AE RMS value and contact load was observed.

Fig. 4 shows the relationship between AE RMS value and the average sliding speed of mechanical seal, which was calculated using the average of the outer and inner diameters of sealing interface. As predicted by Eq. (25), the AE RMS has a square root relationship with sliding speed ($R^2 = 0.99$).

The relationships observed from this experimental study were also validated by tests conducted in the R&D laboratory at John Crane.

4. Conclusion

The paper developed a model of the acoustic emission generated by material elastic asperity contact. The model shows that the level of AE measurement is determined by the load supported by asperity contact, sliding speed, the number of asperity contact and surface topographic characteristics. The relationship was validated by the experimental study conducted on the test rig for the condition monitoring of mechanical seals. On the basis of this model, the contact load between seal face, which is a key factor in the safe operation of mechanical seals, is possible to be predicted by AE measurement when the sliding speed is known. The success of the experiment demonstrated the potential of the developed model to detect and evaluate the premature failure of machinery at an early stage.

Acknowledgement

Appendix A. Appendix: Nomenclature

A_o	the apparent contact area.
D_{SUM}	the asperity density
E'	the Hertzian contact modulus
G	the electrical conductance of the AE measuring circuit
$P(z)$	the probability of randomly variable z
R'	the radius of the curvature in the Hertzian contact area
R_q	mean root square surface roughness
U_{AE}	the energy of acoustic emission signal
U_{iE}	the elastic energy stored in individual asperity contact
$\dot{U}_E$	the elastic energy release rate of asperity contacts
$\dot{U}_{AE}$	the energy rate of acoustic emission caused by total asperity contacts
$\dot{U}_{iAE}$	the elastic energy rate released by individual asperity contact
$\overline{U}_{iE}$	the mean elastic energy stored in asperity contact
$V(t)$	the measured AE electrical signal
V_{rms}	the RMS value of AE signal
W	the normal load on a surface
a	the radius of Hertzian contact area
d	separation between reference plans of rough surfaces
$f(z)$	the probability density function (PDF) of randomly variable z
h	the standardized separation
k_e	the portion of the elastic strain energy converts to acoustic emission pulses
k_m	the gain of the AE measurement system
k_c	$k_c = \frac{2k_e k_m}{5}$
k_s	$k_s = \sqrt{k_c}$
v	the average sliding speed of the face
$z(x)$	the height of the surface profile from the mean line at a distance x

Greek symbols

δ	the maximum Hertzian deflection
$\phi(s)$	the standardized height distribution
σ	the standard deviation of distribution
τ	the release time of the individual asperity elastic energy
$\bar{\tau}$	the mean release time of the individual asperity elastic energy
υ_1, υ_2	the Poisson's ratios of the contact materials

References

[1] R.J. Boness, S.L. McBride, Adhesive and abrasive wear studies using acoustic emission techniques, Wear 149 (1991) 41–53.

[2] R.J. Boness, Measurements of wear and acoustic emission from fuel-wetted surfaces, Wear 162–164 (1993) 703–705.

[3] J. Sun, R.J.K. Wood, L. Wang, I. Care, H.E.G. Powrie, Wear monitoring of bearing steel using electrostatic and acoustic emission techniques, Wear 259 (2005) 1482–1489.

[4] S. Lingard, C.W. Yu, C.F. Yau, Sliding wear studies using acoustic emission, Wear 162–164 (1993) 597–604.

[5] K. Matsuoka, D. Forrest, M.K. Tse, On-line wear monitoring using acoustic emission, Wear 162–164 (1993) 605–610.

[6] J. Hanchi, B.E. Klamecki, Acoustic emission monitoring of the wear process, Wear 145 (1991) 1–27.

[7] G.A. Sarychev, V.M. Shchavelin, Acoustic emission method for research and control of friction pairs, Tribology International 24 (1991) 11–16.

[8] L. Wang, R.J.K. Wood, Acoustic emission from lubricated hybrid contacts, Tribology International 42 (2009) 1629–1637.

[9] J. Miettinen, V. Siekkinen, Acoustic emission in monitoring sliding contact behaviour, Wear 181–183 (1995) 897–900.

[10] F.P. Bowden, D. Tabor, Friction and Lubrication of Solids, Oxford University Press, 1950.

[11] J.F. Archard, Elastic deformation and the laws of friction, Proceedings of the Royal Society of London Series A 243 (1957) 190–205.

[12] J.A. Greenwood, J.B.P. Williamson, Contact of nominally flat surfaces, Proceedings of the Royal Society of London Series A 295 (1966) 300–319.

[13] D. Maugis, Contact, Adhesion and Rupture of Elastic Solid, Springer, 2000.

[14] Y. Fan, Condition monitoring of mechanical seals using acoustic emissions, PhD thesis, The University of Manchester, 2007, pp. 155–171.